

Pelvic Endometriosis: Detection and Diagnosis with Chemical Shift MR Imaging¹

Fat-saturation magnetic resonance (MR) imaging for detection and characterization of pelvic endometriosis was prospectively investigated in 35 women with a clinical diagnosis of the disease. Large endometrioma was diagnosed when the lesion was larger than 1 cm in diameter and hyperintense on T1- and T2-weighted images. Small endometrioma was diagnosed when a well-demarcated hyperintense lesion less than 1 cm in diameter was seen on T1-weighted or fat-saturated T1-weighted images. Surgery performed after MR imaging revealed a normal pelvis in six patients, endometriosis in 26 (33 large and 19 small endometriomas), and other cystic lesions in three. Conventional T1- and T2-weighted imaging accurately demonstrated 27 of 33 large endometriomas and two of 19 small endometriomas. Fat-saturation T1-weighted imaging in combination with conventional technique accurately demonstrated 30 of 33 large and nine of 19 small endometriomas. Diagnostic accuracy was improved with addition of fat-saturated images, so their use together with conventional images is recommended in assessment of endometriosis.

Index terms: Endometriosis, 791.318, 83.3192, 85.3192 • Gastrointestinal tract, abnormalities, 791.318 • Genitourinary system, abnormalities, 83.3192, 85.3192 • Magnetic resonance (MR), chemical shift • Ovary, neoplasms, 852.3192 • Pelvic organs, diseases, 85.3192

Radiology 1993; 188:435-438

¹ From the Departments of Radiology (K.S., H.O., I.I., Y.K., T.I.) and Obstetrics and Gynecology (K.T., M.K.), Shimane Medical University, 89-1 Enya, Izumo 693, Japan. Received November 18, 1992; revision requested January 12, 1993; final revision received March 25; accepted March 29. Address reprint requests to K.S.

© RSNA, 1993

ENDOMETRIOSIS is a condition in which functioning endometrial glands and stroma develop outside their normal location (1). The most common sites of involvement are intraperitoneal, and in descending order of frequency, they include the ovaries, uterine ligaments, pouch of Douglas, pelvic peritoneum covering the uterus, fallopian tubes, rectosigmoid region, and urinary bladder (1-3).

Magnetic resonance (MR) imaging has been advocated as the modality of choice for evaluation of endometriosis (4-10), although some limitations in detection of small peritoneal masses have been pointed out (4,7,9). Nevertheless, the hope that MR imaging may obviate laparoscopy has also been expressed (4,7-9).

Fat-saturation techniques can be used to decrease chemical shift artifact in structures surrounded by fat and to decrease phase artifact in the upper abdomen, through reduction of the signal intensity of the respiration-induced motion of subcutaneous fat (11,12). It has also been reported that fat-saturation techniques were useful to improve the distinction between blood and lipid within ovarian masses (10).

This prospective study was designed to analyze the value of MR imaging in the detection and characterization of pelvic endometriosis. We assessed the usefulness of fat-saturation MR imaging for the detection of endometrial cysts, with laparoscopy or laparotomy as the standard of reference.

MATERIALS AND METHODS

This prospective study was conducted between March 1991 and August 1992. Thirty-five consecutive women aged 24-48 years (mean, 36 years) with clinically suspected endometriosis were referred for MR imaging. In all patients, surgery was performed no later than 2 weeks after MR imaging. MR images were compared with the results of laparoscopy in 13 patients and with laparotomy findings in the other

22 patients. Laparoscopy and laparotomy procedure reports, photographs obtained during the procedures, and histologic slides (when available) were reviewed by two gynecologists from our university.

MR imaging was performed with a 1.5-T superconducting magnet (Signa; GE Medical Systems, Milwaukee, Wis). Spin-echo T1-weighted (600/15) (repetition time msec/echo time msec) and T2-weighted (2,000/80) images and fat-saturated T1-weighted images (600/15) were obtained in all patients. The 600/15 images were obtained in the axial plane with a 256 × 256 matrix and two signals averaged. The section thickness was 6 mm, with a 2-mm intersection gap. Inferior and superior saturation pulses were applied. These parameters were kept as similar as possible for both the regular spin-echo and fat-saturated images.

The MR images were prospectively read by two of the authors (K.S., H.O.) with the knowledge that the patient had a clinical history of suspected endometriosis. They specifically recorded (a) the lesion location, size, and shape; (b) the thickness, regularity, and signal intensity of the lesion margins; (c) the distinctness of the interface of the lesion with adjacent organs; and (d) the appearance of the lesions (ie, homogeneity and signal intensity of each lesion compared with that of adjacent adipose tissue and striated muscle).

Large endometrioma was diagnosed when the mass was 1 cm or larger in diameter. A "definitive" diagnosis of large endometrioma was made when a mass that was entirely hyperintense on T1-weighted images or fat-saturated T1-weighted images exhibited hypointense signal (usually mixed with hyperintense areas) on T2-weighted images ("shading") or when the lesion consisted of multiple entirely hyperintense cysts on T1-weighted or fat-saturated T1-weighted images ("multiplicity"), regardless of the signal intensity on T2-weighted images. A "suggestive" diagnosis was made for masses that were hyperintense on T1-weighted or fat-saturated T1-weighted images and exhibited homogeneous hyperintensity on T2-weighted images (9). In the evaluation of ovarian endometrioma, tiny lesions that were considered to be endometrial masses were excluded from this classification.

Small endometriomas were diagnosed when high-signal-intensity lesions 1 cm or smaller in diameter were demonstrated on T1-weighted or fat-saturated T1-weighted images (7). For MR imaging-surgical correlation of sites of involvement, the pelvis was divided into five regions: the surface of the uterus, the right and left adnexae, the pouch of Douglas, and the peritoneum.

The numbers of small and large endometrioma detected with fat-saturation imaging and conventional imaging were compared by using χ^2 analysis.

RESULTS

Overall Accuracy

Laparoscopy or laparotomy revealed a normal pelvis in six of the 35 patients. Of the remaining 29 patients, 26 had surgically established endometriosis and a total of 52 lesions, including 33 large endometriomas (ovarian endometrial cystic masses) and 19 small endometriomas. The other three patients had hematosalpingitis, benign cystic teratoma, and ovarian cancer with internal hemorrhage.

The two independent observers agreed on the MR imaging analysis for 32 of the 35 patients, and a consensus was arrived at in the other three. In all three of the latter patients, misperceptions of anatomic abnormalities were clarified at the conference reading.

The lack of abnormalities in six patients was recognized on conventional T1- and T2-weighted images. The diagnosis was not changed by adding the fat-saturated T1-weighted images.

Among the 26 patients with endometriosis, MR imaging with conventional T1- and T2-weighted sequences indicated endometriosis in 19 and a

normal pelvis in seven. When fat-saturated images were used, six patients had a normal pelvis and 20 had endometriosis. Two patients had only adhesions and five had only small endometriomas. Therefore, the overall sensitivity, specificity, and accuracy were 73%, 67%, and 71%, respectively, for T1- and T2-weighted images, and 77%, 78%, and 77%, respectively, for all three types of images.

Ovarian Endometriomas

At surgery, 33 large ovarian endometriomas were detected. At histologic examination, one of the 33 was found to contain an ovarian carcinoma. Also, surgery disclosed hydrosalpinx in two patients and a simple cyst in one.

MR imaging with conventional T1- and T2-weighted sequences permitted identification of 27 of 33 large endometriomas (Figs 1–3). Two diagnoses were suggestive and 25 were definitive, with the sensitivity being 82%, the specificity being 91%, the

positive predictive value being 90%, and the negative predictive value being 84%, with the suggestive diagnoses included. With all three types of MR images, 30 endometriomas could be identified. Three diagnoses were suggestive and 27 were definitive, so the sensitivity was 91%, the specificity was 94%, the positive predictive value was 94%, and the negative predictive value was 92%. Statistically significant differences between detection schemes were not shown with the χ^2 test.

On T1-weighted images, hyperintensity was noted in 21 lesions, intermediate intensity in 10, and predominantly low signal intensity in two. The latter two were misdiagnosed as other adnexal masses. On fat-saturated T1-weighted images, six of 10 lesions with intermediate intensity on conventional T1-weighted images showed high signal intensity, because the dynamic range became more narrow and therefore allowed depiction of subtle differences with greater conspicuity and therefore a diagnosis of endometriosis (Fig 3). Six lesions,

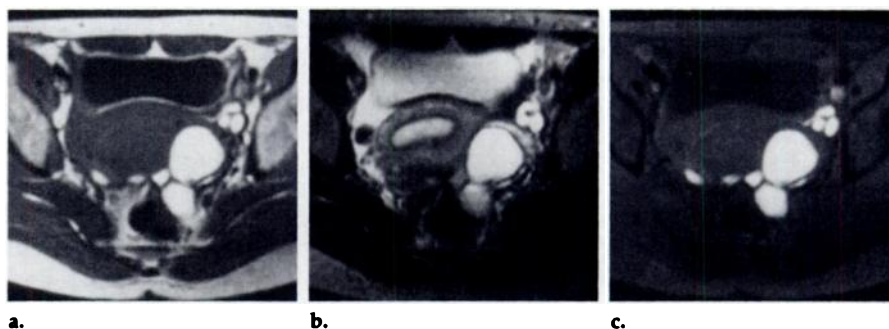


Figure 1. (a) T1-weighted (600/15), (b) T2-weighted (2,000/80), and (c) fat-saturated T1-weighted (600/15) MR images depict an endometrioma in a 34-year-old woman. The T1- and T2-weighted images show a high-signal-intensity cyst with multiplicity. On the fat-saturated image, multiplicity is demonstrated more accurately, and small endometriomas are clearly seen on the posterior surface of the uterus.



Figure 2. (a) T1-weighted (600/15), (b) T2-weighted (2,000/80), and (c) fat-saturated T1-weighted (600/15) MR images depict multiple endometrial cysts in a 38-year-old woman. The lesions show high signal intensity on T1-weighted and fat-saturated T1-weighted images (multiplicity). On the T2-weighted image, one cyst exhibits low signal intensity with areas of high signal intensity (arrow), and a normal follicle (arrowhead) is evident.

however, did not show high signal intensity on fat-saturated T1-weighted images (false-negative). These endometriomas were filled with clotted or fresh blood at surgery. Multiplicity was noticed on T1-weighted images in 17 cases and on fat-saturated T1-weighted images in 22 (Fig 1). In 20 patients, shading was noticed on T2-weighted images (Fig 2). With conventional T1- and T2-weighted imaging, 12 lesions demonstrated both criteria for a definitive diagnosis (shading and multiplicity), and 14 lesions did so when fat-saturated T1-weighted images were added.

A hematosalpinx, a cystic teratoma, and an ovarian carcinoma with internal hemorrhage were given a suggestive diagnosis of endometriosis on T1- and T2-weighted images (false-positive results). There were no hemorrhagic cysts in our study. On fat-saturated T1-weighted images, the cystic teratoma was correctly diagnosed from its decreased signal inten-

sity, but fat saturation did not allow diagnosis of the other two hemorrhagic lesions (Fig 4).

Small Endometriomas

At surgery, 19 small endometriomas were revealed (four lesions in the uterine serosal surface, 11 in the ovaries, and four others in intraperitoneal locations). In two patients with a closed pouch of Douglas and five patients with ovarian endometrioma, however, small endometriomas could not be assessed. Conventional T1- and T2-weighted imaging depicted only two of 19 small endometriomas (in the left sacrouterine ligament and left ovary). On conventional images, most of the small endometriomas could not be defined because their signal intensity was similar to that of fat. The addition of fat-saturated T1-weighted images increased detection to nine small endometriomas (one in the

uterine serosal surface, six in the ovaries, and two in other intraperitoneal areas) (Fig 5). Thus, the sensitivity was 11%, the specificity was 98%, the positive predictive value was 33%, and the negative predictive value was 90% with conventional T1- and T2-weighted images, while the respective values were 47%, 97%, 64%, and 94% when fat-saturated T1-weighted images were added. The difference in sensitivity between conventional T1-weighted imaging and fat-saturation T1-weighted imaging approached a significant level ($P < .01$). On fat-saturated T1-weighted images, two lesions in the pouch of Douglas and two ovarian lesions were suspected, but the pouch was closed at laparoscopy, so these lesions could not be confirmed.

DISCUSSION

Endometriosis is defined as the presence of endometrial epithelium and stroma in an ectopic site outside the uterine cavity (1). This disease is difficult to diagnose, stage, and manage. Confirmation of the diagnosis by means of laparoscopy (or laparotomy, if indicated) is usually considered necessary before commencement of therapy. Endometriosis should be staged to determine the appropriate treatment and assess the prognostic factors. Surgical staging is performed according to a point system, which is based on the presence, size, and location of the endometrial masses and presence and type of adhesions (1–3).

Ultrasound (US) (13–17) and computed tomography (CT) (18,19) have been proposed as imaging modalities for diagnosis of endometriosis. Most US (13–15) and CT (18,19) studies, however, have only addressed the detection of endometriomas in the differential diagnosis of a pelvic mass and did not consider the more common, diffuse form of

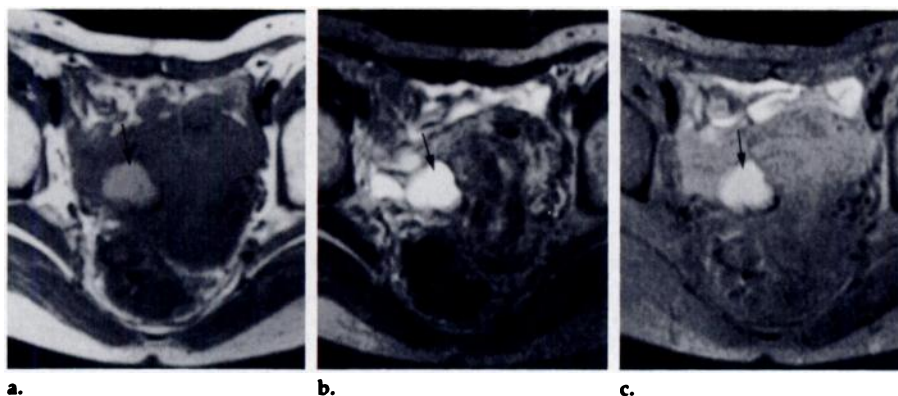


Figure 3. (a) T1-weighted (600/15), (b) T2-weighted (2,000/80), and (c) fat-saturated T1-weighted (600/15) MR images show an endometrial cyst in a 43-year-old woman. A right ovarian lesion (arrow) shows slightly low signal intensity relative to subcutaneous tissue on the T1-weighted images and high signal intensity on the T2-weighted image. On the fat-saturated T1-weighted image, signal intensity of the lesion is exclusively high, and a “suggestive” diagnosis could be made.

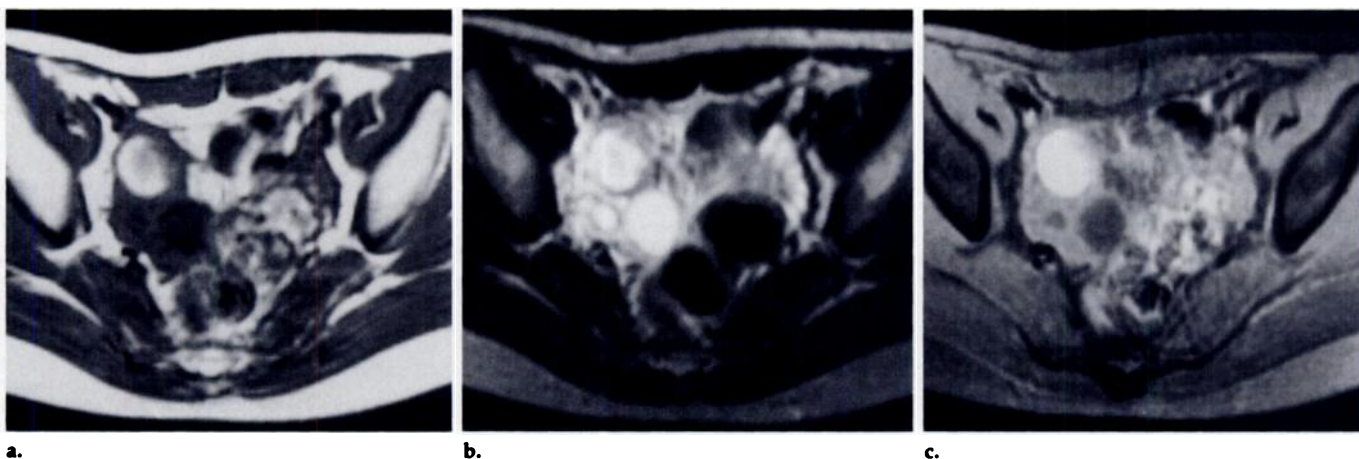


Figure 4. (a) T1-weighted (600/15), (b) T2-weighted (2,000/80), and (c) fat-saturated T1-weighted (600/15) MR images obtained in a 24-year-old woman in whom hematosalpingitis was identified at surgery. The right adnexal cyst exhibits high signal intensity on the fat-saturated image and mimics an endometrial cyst. Surgery revealed hematosalpingitis of the right adnexa.

endometriosis. In a study by Friedman et al (16), US depicted endometriosis in only four of 37 patients (11%). CT is clearly of little value in this disorder, since the contrast resolution is insufficient to distinguish endometriomas from the normal adnexae (18,19).

With regard to the detection of endometriomas with conventional T1- and T2-weighted MR imaging, Arrive et al (7) reported a sensitivity of 88% and Zawin et al (8) reported a sensitivity of 71% and a specificity of 82%. In our study, conventional T1- and T2-weighted images achieved a sensitivity of 82% and a specificity of 91%. Fat-saturated T1-weighted images can clearly make hyperintense lesions more conspicuous, but in most cases, they can be seen on conventional images. Therefore, use of supplemental fat-saturated T1-weighted images did not significantly increase the sensitivity for large endometriomas. Four of 10 lesions for which conventional images did not allow a diagnosis of endometriomas were diagnosed as such with fat-saturated images because the more narrow dynamic range showed subtle differences with greater conspicuity. Conventional images showed multiplicity in 17 lesions, while fat-saturated T1-weighted images showed multiplicity in 22 lesions. Thus, the fat-saturation technique improved depiction of the detailed structure of endometriomas.

Previous reports have described the main limitation of MR imaging as its lack of sensitivity for detecting small endometriomas (4-10). In our study, the sensitivity was only 11% with conventional T1- and T2-weighted images. On conventional images, almost all small endometriomas could not be detected because of pelvic adipose tissues. Contrast between small endometriomas and the adipose tissue surrounding normal organs and the pelvic serosa may be insufficient for clear depiction of small endometriomas. Addition of fat-saturated T1-weighted images increased the sensitivity to 47% and significantly improved the depiction of small endometriomas in the pelvis. Ten of 19 small endometriomas, however, were still not detected. The following reasons for the lack of visualization can be suggested. Because small endometriomas can exhibit varying degrees of hemorrhage due to hormonal stimulation, the appearance may vary, depending on the age of the hemorrhage (1). Some false-negative lesions showed chronic hemorrhage and demonstrated low signal intensity due to the presence of hemosiderin (20,21). Furthermore, small endometriomas are often too small for current MR imaging resolution; many on the uterine serosal surface are as small as 1 mm in diameter (7). In addition, peristalsis may blur the tissue planes, and bowel loops (which can show vari-

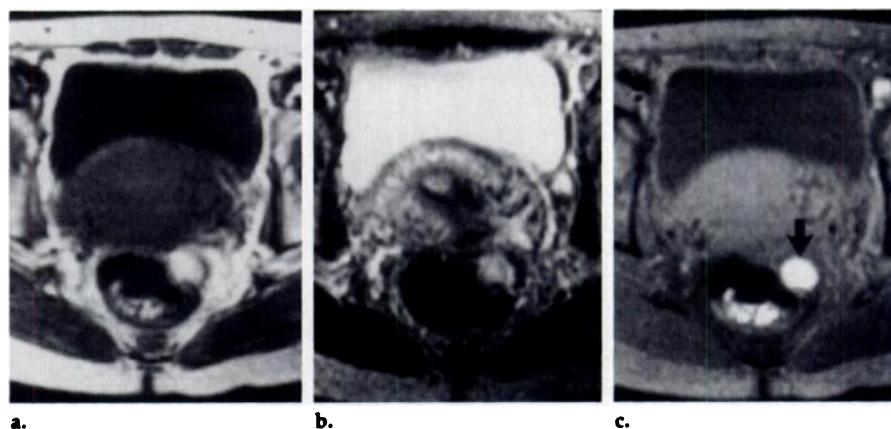


Figure 5. (a) T1-weighted (600/15), (b) T2-weighted (2,000/80), and (c) fat-saturated T1-weighted (600/15) MR images obtained in a 34-year-old woman with a small endometrioma. On the fat-saturated T1-weighted image, the small endometrioma is evident on the serosa of the sigmoid colon (arrow in c). On T1- and T2-weighted images, the lesion was not detected because of adipose tissue.

ous signal intensities) adjacent to the peritoneal surface may mimic or obscure a small endometrioma (7). Finally, the 6-mm section thickness used in our study may have contributed to difficulty in identification of small implants. With a 5-mm section thickness, however, Nishimura et al (4) were also unable to depict small peritoneal lesions.

The limited ability of conventional MR imaging to demonstrate small masses was improved by use of the fat-saturation technique, but the absence of a correlation between MR imaging findings and disease severity still remains. The small fibrotic blebs composed primarily of fibrosis and hemosiderin with little or no fluid can only be detected at laparoscopy. Hemorrhagic cysts, hemorrhagic tumors, and, occasionally, high signal intensity within the bowel lumen may be difficult to distinguish from endometriomas. In view of these limitations, we believe laparoscopy remains the procedure of choice for the primary evaluation of endometriosis. Laparoscopy occasionally fails to reveal lesions hidden by adhesions, however, so both MR imaging with fat saturation and laparoscopy may have a place in the evaluation of endometriosis. ■

References

- Clement PB. Endometriosis, lesions of the secondary müllerian system, and pelvic mesothelial proliferations. In: Kurman RJ, ed. *Blaustein's pathology of the female genital tract*. 3rd ed. New York, NY: Springer-Verlag, 1987; 516-559.
- Williams TJ. Endometriosis. In: Mattingly RF, Thompson JD, eds. *Te Linde's operative gynecology*. 6th ed. Philadelphia, Pa: Lippincott, 1985; 257-286.
- Rock JA. Endometriosis. In: Rasenwaks Z, Benjamin F, Stone ML, eds. *Gynecology: principles and practice*. New York, NY: Macmillan, 1987; 559-576.
- Nishimura K, Togashi K, Itoh K, et al. Endometrial cyst of the ovary: MR imaging. *Radiology* 1987; 162:315-318.
- Mitchell DG, Mintz MC, Spritzer CE, et al. Adnexal masses: MR imaging observations at 1.5 T with US and CT correlation. *Radiology* 1987; 162:319-324.
- Nyberg DA, Porter BA, Olds MO, Olson DO, Anderson R, Wesby GE. MR imaging of hemorrhagic adnexal masses. *J Comput Assist Tomogr* 1987; 11:664-669.
- Arrive L, Hricak H, Martin MC. Pelvic endometriosis: MR imaging. *Radiology* 1989; 171:687-692.
- Zawin M, McCarthy SM, Scoutt L, Comite F. Endometriosis: appearance and detection at MR imaging. *Radiology* 1989; 171:693-696.
- Togashi K, Nishimura K, Kimura I, et al. Endometrial cyst: diagnosis with MR imaging. *Radiology* 1991; 180:73-78.
- Kier R, Smith RC, McCarthy SM. Value of lipid- and water-suppression MR images in distinguishing between blood and lipid within ovarian masses. *AJR* 1992; 158:321-325.
- Mitchell DG, Vinitski S, Saponaro S, Tasciyan T, Burk DL Jr, Rifkin MD. Liver and pancreas: improved spin-echo T1 contrast by shorter echo time and fat suppression at 1.5 T. *Radiology* 1991; 178:67-71.
- Semelka RC, Kroeker MA, Shoenut JP, Kroeker R, Yaffe CS, Micflikier AB. Pancreatic disease: prospective comparison of CT, ERCP, and 1.5-T MR imaging with dynamic gadolinium enhancement and fat suppression. *Radiology* 1991; 181:785-791.
- Coleman BG, Arger PH, Mulhern CB Jr. Endometriosis: clinical and ultrasonic correlation. *AJR* 1979; 132:747-749.
- Walsh JW, Taylor KJW, Rosenfield AT. Gray scale ultrasonography in the diagnosis of endometriosis and adenomyosis. *AJR* 1979; 132:87-90.
- Walsh JW, Taylor KJW, Wasson JFM, Schwartz PE, Rosenfield AT. Gray-scale ultrasound in 204 proved gynecologic masses: accuracy and specific diagnostic criteria. *Radiology* 1979; 130:391-397.
- Friedman H, Vogelzang RL, Mendelson EB, Neiman HL, Cohen M. Endometriosis detection by US with laparoscopic correlation. *Radiology* 1985; 157:217-220.
- Berland LL, Lawson TL, Albarelli JN, Foley WD. Ultrasonic diagnosis of ovarian and adnexal disease. *Semin Ultrasound* 1980; 1:17-29.
- Fishman EK, Scatarige JC, Saksouk FA, Rosenheim NB, Siegelman SS. Computed tomography of endometriosis. *J Comput Assist Tomogr* 1983; 7:257-264.
- Sawyer RW, Walsh JW. CT in gynecologic pelvic disease. *Semin Ultrasound CT MR* 1988; 9:122-142.
- Gomori JM, Grossman RI, Goldberg HI, Zimmerman RA, Bilaniuk LT. Intracranial hematomas: imaging by high-field MR. *Radiology* 1985; 157:87-93.
- Gomori JM, Grossman RI, Hackney DB, Goldberg HI, Zimmerman RA, Bilaniuk LT. Variable appearance of subacute intracranial hematomas on high-field spin-echo MR. *AJNR* 1987; 8:1019-1026.